

A QoS-Aware Uplink Spectrum and Power Allocation with Link Adaptation for Vehicular Communications in 5G networks

Krishna Pal Thakur, Basabdatta Palit, *Member, IEEE*

Abstract—In this work, we have proposed link adaptation-based joint spectrum and power allocation algorithms for the uplink communication in 5G Cellular Vehicle-to-Everything (C-V2X) systems. In C-V2X, vehicle-to-vehicle (V2V) users share radio resources with vehicle-to-infrastructure (V2I) users. Existing works primarily focus on the optimal pairing of V2V and V2I users, assuming that each V2I user needs a single resource block (RB) while minimizing interference through power allocation. In contrast, in this work, we have considered that the number of RBs needed by the users is a function of their channel condition and Quality of Service (QoS) - a method called link adaptation. It effectively compensates for the frequent channel quality fluctuations at the high frequencies of 5G communication. 5G uses a multi-numerology frame structure to support diverse QoS requirements, which has also been considered in this work.

The first algorithm proposed in this article greedily allocates RBs to V2I users using link adaptation. It then uses the Hungarian algorithm to pair V2V with V2I users while minimizing interference through power allocation. The second proposed method groups RBs into resource chunks (RCs) and uses the Hungarian algorithm twice - first to allocate RCs to V2I users and then to pair V2I users with V2V users. Extensive simulations reveal that link adaptation increases the number of satisfied V2I users and their sum rate while also improving the QoS of V2I and V2V users, making it indispensable for 5G C-V2X systems.

Index Terms—Resource Allocation, Vehicle-to-Vehicle, C-V2X, 5G, Link Adaptation, 28GHz, Hungarian, Multi-Numerology

I. INTRODUCTION

In recent times, Cellular Vehicle-to-Everything (C-V2X) communication has emerged as a key enabler for intelligent, automated, safe, and green vehicular communications. C-V2X services consist of - 1) communication between vehicles and the mobile network (Vehicle-to-Infrastructure (V2I)), and 2) direct communication between vehicles (Vehicle-to-Vehicle (V2V)). V2I communication includes the exchange of road traffic and safety messages as well as other infotainment services such as voice and video calling, multimedia streaming, etc. V2V communication, on the other hand, is mostly targeted towards improving road safety. Therefore, the Quality of Service (QoS) requirements, such as latency and reliability, of V2V messages are stricter than their V2I counterparts. For example, the Block Error Rate (BLER) requirement of V2I users is 0.1, while that of V2V users is 0.001 [1]. Although 5G New Radio (NR) supports C-V2X communication [2, 3],

such diverse QoS provisioning over 5G mmWave vehicular networks is challenging due to the high frequency of operation. One possible solution is designing and implementing efficient radio resource allocation schemes for 5G C-V2X (NR-V2X) communication, which is addressed in this work.

5G uses Orthogonal Frequency Division Multiple Access (OFDMA), in which the spectrum is partitioned into orthogonal time-frequency Resource Blocks (RBs). Conventionally, in 4G, all OFDMA RBs have a uniform bandwidth and time duration. However, as services are expected to diversify further in 5G, such a uniform numerology may not suffice [4]. Hence, to support the different QoS requirements in 5G, 3GPP prescribes the use of multiple numerologies [5–8], where each numerology is characterized by a different bandwidth and time duration of the RBs. A popular method of using these multiple numerologies is to slice the system bandwidth into orthogonal parts and assign a different numerology to each part. Users are assigned to these Bandwidth Parts (BWPs) based on which numerology caters to their QoS requirements. Hence, while designing resource allocation methods for 5G C-V2X systems, it becomes imperative to account for multiple numerologies.

Another important aspect in the resource allocation in C-V2X systems is how V2I users share the RBs with V2V users. C-V2X extensively leverages the existing cellular network infrastructure for V2I communications. The V2V services, on the other hand, are provided either in 1) *the underlay Device-to-Device (D2D) communication* mode [9] in which V2V users coexist in the RB of a V2I user, or 2) *the dedicated mode* where V2V users are assigned exclusive resources [10, 11]. The former offers an efficient use of radio resources but suffers from interference between the V2I and V2V users. To minimize this interference, efficient power control techniques are used in the shared frequency resource, which helps to achieve a higher sum rate and satisfy the required QoS.

An inherent assumption in existing works on resource allocation in C-V2X networks [9–30] is that each V2I user needs one RB. This ignores the basic premise of radio resource allocation, which is compensating for the underlying channel impairments [1]. Allocating a single RB implies that all the users can use the same Modulation and Coding Scheme (MCS), and their channel condition is reasonably good. Let us consider an example. A V2I user needs to transmit a 50-byte packet in one time slot such that the BLER is 0.1. This packet can be sent using a single RB of bandwidth 1440 HZ only when the modulation scheme is 16 QAM [1, Table 3]. Such a high modulation scheme can be achieved when the

K.Pal Thakur is with the Department of Electronics and Telecommunication Engineering, IEST Shibpur, Howrah - 71103, West Bengal, India.

B.Palit is with the Department of Electronics and Communication Engineering, NIT Rourkela, Rourkela - 769008, Odisha, India.

Signal-to-Interference-Plus-Noise-Ratio (SINR) is at least as high as 11.4 dB [1], which may not always be achievable. For a user experiencing a lower SINR, a lower MCS can be supported, and, hence, multiple RB would be needed. The resource allocation algorithm can wait for the link condition to improve until only a single RB is required, affecting the timeliness of message delivery. On the other hand, Adaptive MCS selection can compensate for the channel impairments - a method called Link Adaptation [31]. In this case, the choice of the MCS, and consequently the number of RBs required, would depend on the user's underlying link condition, the amount of data to transmit at a time, and the requested QoS. To the best of the authors' knowledge, this aspect is amiss in existing works on multi-numerology-based resource allocation in 5G vehicular communications. So, in this work, we argue that a combination of link-adapted resource allocation, power allocation, and resource sharing in a multi-numerology setup is imperative to provide improved sum rates and QoS to different types of users in a 5G C-V2X communication system.

The objective in this work is to use a link adaptation based spectrum allocation and power allocation in the uplink to maximize the number of V2I users and their sum rates while conforming to the QoS guarantees of the V2I and V2V users. The QoS guarantees are specified by outage probability constraints, average packet delays, and BLER requirements. Due to link adaptation, the number of RBs allocated to each user becomes a variable quantity, thereby making the resource sharing between V2I and V2V users more challenging. In addition, we have also considered the presence of multiple best-effort users along with V2I and V2V users. To support such diverse QoS requirements, we have used multiple numerologies [5]. We have, thus, reformulated the problem of spectrum and power allocation in C-V2X communication for 5G networks, wherein we have not only considered the pairing between V2I users and underlaid V2V users but also the link adaptation based resource allocation in a multi-numerology setup. The proposed method offers a more comprehensive and practical approach towards resource allocation in 5G C-V2X. The major contributions are:

- 1) We have proposed two resource allocation algorithms for V2I and V2V users in the shared mode.
 - a) The first algorithm, *Greedy Resource Allocation with Hungarian Sharing (GRAHS)* operates as follows. - (i) First, it greedily allocates RBs to V2I users through an adaptive selection of MCSs. (ii) It then allocates power to all the V2I and V2V user pairs, in the RBs that are assigned to the respective V2I user in step (i), such that the V2I datarate is maximized. (iii) Using the new power allocation from step (ii), GRAHS pairs the V2I and V2V users using the Hungarian algorithm such that the respective QoS requirements and outage probability conditions are satisfied [17, 21, 32].
 - b) As GRAHS allocates non-contiguous resources, hence we have also proposed a second algorithm, *called Hungarian Resource Allocation with Hungarian sharing (HRAHS)*, to maximize the V2I datarate. This algorithm groups a set of RBs as a Resource Chunk (RC)

[33, 34] and assigns these RCs to the V2I users using the Hungarian algorithm. This is followed by another Hungarian algorithm, which pairs the scheduled V2I and the V2V users.

- 2) We have also explored the dedicated or overlay mode [10, 11] in which V2I and the V2V users are assigned orthogonal resources. We have compared the three algorithms - GRAHS, HRAHS, dedicated mode of resource allocation - in terms of their real-time traffic capacity and sum rate. We have defined the real-time traffic capacity as the number of V2I users for which at least 95% users have -1) a packet loss rate less than 2%, and 2) average packet delay less than the delay bound [35].

Extensive simulations and comparison with an existing work [24] show that link adaptation increases the number of supported V2I users by nearly five times when it is used in dedicated mode and seven times when link adaptation is used in the shared mode.

The rest of the article is organized as follows. Section II discusses the related work. Section III explains the system model and problem formulation. Section IV describes the proposed algorithms. Section V discusses the results obtained. Section VI concludes the article.

II. RELATED WORK

This section discusses the existing works on resource and power allocation in C-V2X systems. These works primarily consider three aspects: (i) spectrum allocation, (ii) spectrum sharing, and (iii) power allocation for interference minimization in shared resources.

The work in [9] proposes a location-information-aided power control technique for D2D-based vehicular communication networks where multiple V2V users share the link of a V2I user in the uplink. The algorithm in [13] allocates power using the difference of two convex functions approach and uses a game theory for V2V clustering. Authors in [16] propose a Deep Reinforcement Learning (DRL) based control aware power and radio resource allocation algorithm for vehicle platoons. The work in [10] considers a mixed mode of resource allocation, in which V2V users either - (i) get dedicated RBs, (ii) or share RBs with the Pedestrian UE (PUE) which directly communicate with the Base Station (BS), (iii) or select the RBs themselves without any involvement of the evolved NodeB (eNB). Authors in [11] extend the work in [10] to include a power allocation for interference control and a low-complexity user-pairing method. The resource allocation algorithm in [12] uses reinforcement learning in graph neural networks to allocate resources to V2V and V2I users while maximizing the sum capacity. The deep learning-based algorithm in [14] takes decisions on resource sharing between V2I and V2Vs users. The work in [15] explores belief propagation and a factor graph model to investigate if multiple V2V links can share the RB assigned to a V2I user. However, [9, 11–16] need full and perfect Channel State Information (CSI) for power and resource allocation. However, the high mobility-induced fast channel strength variations cause Doppler Spread, delaying instantaneous CSI feedback.

Table I: Summary of Recent Works on Spectrum Allocation in C-V2X Networks and Comparison with the Current Work

References	Summary	Power Allocation	Resource Allocation	Resource Sharing	QoS Awareness	Imperfect CSI	Link Adaptation
[9]	Proposes a location information-aided power control mechanism to reduce interference in the reused channel for V2V communication over underlaid D2D links.	✓	×	✓	×	×	×
[10]	Studies three resource allocation modes for VUEs - eNB assisted dedicated and shared modes, and distributed or autonomous mode; proposes a joint resource mode selection and resource allocation scheme.	×	✓	✓	×	×	×
[11]	Extends [10] to include power allocation to reduce interference between V2V users and PUEs.	✓	✓	✓	×	×	×
[12]	Proposes a resource allocation algorithm that uses a reinforcement learning-based GNN framework for resource sharing between V2V and V2I users to maximize the sum-capacity.	×	✓	✓	×	×	×
[13]	Proposes a resource allocation scheme in which one V2I link is shared by multiple V2Vs users. V2V pairs are clustered using coalition games, and power allocation is used to minimize interference.	✓	×	✓	×	×	×
[14]	Proposes a power allocation and a belief propagation-based RB allocation in which multiple V2V links share RBs; RBs are allocated to maximize sum capacity.	✓	✓	✓	×	×	×
[15]	Proposes a deep learning-based spectrum reuse and power allocation scheme.	✓	×	✓	×	×	×
[17]	Proposes a power allocation and spectrum sharing method for coexisting V2I and V2V users to maximize the sum-ergodic capacity and the minimum ergodic capacity of the V2I users while satisfying the minimum link guarantees for V2V users; uses the Hungarian algorithm to pair V2I and V2V users.	✓	×	✓	✓	×	×
[18]	Proposes a power allocation and spectrum reuse policy that taps large-scale fading information to maximize sum ergodic capacity of V2V and V2I users; analyses packet sojourn time.	✓	×	✓	✓	×	×
[19]	Uses the theory of effective capacity on the large scale fading information to propose a joint power allocation and spectrum reuse method which maximizes the sum ergodic capacity within the constraints of the delay violation probability for V2I and V2V users.	✓	×	✓	✓	×	×
[20]	Extends the work in [18] to include packet retransmission so that the reliability of the transmission can be increased; analyses the packet delay and packet sojourn time using queueing theory.	✓	×	✓	✓	×	×
[21]	Proposes a heuristic method for non-orthogonal resource sharing and power allocation between V2I and V2Vs users, considering the availability of slowly varying CSI while guaranteeing latency and reliability.	✓	×	✓	✓	×	×
[22]	Considers a limited availability of accurate CSI; Uses centralized Hungarian algorithm to assign resources to V2I users and distributed DRL for power control and resource sharing between V2I and V2V users.	✓	✓	✓	×	✓	×
[23]	Uses probabilistic information on CSI for resource allocation of V2I users, power control and subsequent resource sharing between V2I and V2V users.	✓	×	✓	✓	✓	×
[24]	Extends the work in [17] to include high mobility conditions where imperfect CSI feedback is available; maximizes the sum capacity while maintaining the link guarantees for V2V users.	✓	×	✓	✓	✓	×
[25]	Proposes to maximize the sum ergodic capacity of all V2V pairs subject to a minimum SINR requirement of V2I links using a low complexity power allocation approach and the Gale Shapley method to pair multiple V2V links with one V2I links.	✓	×	✓	✓	✓	×
[29]	Uses large-scale fading information to propose a power control and subcarrier assignment algorithm for V2V and V2I users such that the number of V2V links is maximized subject to the diverse QoS requirements of V2I and V2V users.	✓	✓	✓	✓	×	×
This work	Proposes link adapted resource allocation for V2I users and a joint power allocation and resource sharing for V2I and V2V users to increase the number of supported V2I users and their sum capacity while conforming to the QoS guarantees of V2I and V2V users.	✓	✓	✓	✓	✓	✓

The need for complete knowledge of the instantaneous CSI of the V2V users is bypassed in [17–20, 36] by using the large-scale fading information. The algorithm in [17] proposes to allocate power and share spectrum based on the large-scale fading to maximize the sum capacity of V2I links while ensuring a minimum coverage probability of V2V users. In [19], the effective capacity theory is applied to large-scale fading to devise a power allocation and spectrum reuse scheme. The work in [36] proposes a power allocation and spectrum sharing algorithm, which applies multi-agent reinforcement learning on large-scale fading information to maximize sum-capacity of V2I users and provide QoS guarantees and secrecy outage guarantees to V2V users. Large-scale fading depends only on user location; hence, the changes in channel gain vary slowly with time. The work in [21] uses a slowly varying CSI, instead of large-scale fading, for non-orthogonal resource

sharing and power allocation between V2I and V2V users. In [18], the algorithm maximizes the sum rate of V2I users while satisfying the delay requirement of V2V users, assuming that the BS knows only the distribution of the small-scale channel fading. The work in [18] is extended in [20] to include packet retransmission. On the other hand, [23] uses the probabilistic information instead of the accurate CSI to allocate radio resources.

Unlike the aforementioned works, imperfect CSI is considered in the works [22, 24–30]. The work in [24] extends the work in [17] wherein the joint spectrum and power allocation algorithm considers delayed CSI feedback. The work in [22] proposes a combination of centralized and distributed resource allocation based on graphs and reinforcement learning. The proposed algorithm uses limited CSI to allocate spectrum to the V2I users, and the V2V users exploit the realistic

Table II: Symbol Definitions

Symbol	Definition	Symbol	Definition
c	index of Cellular User-Equipments (CUEs)	γ_i^n	SINR of UE i in the RB n , $i \in \{c, v\}$
v	index of Vehicular User-Equipments (VUEs)	R_c	Rate of CUE c
m	index of Best-effort User-Equipments (BUEs)	ρ_c^n	Resource Block allocation variable
δ_i	Time-to-live of packets of user type i , $i \in \{c, v\}$	$x_{c,v}$	Resource Sharing indicator variable
β_i	Packet Size of user type $i \in \{c, v\}$	η_c^n	Resource Chunk Allocation variable for HRAHS
\mathcal{B}_i	Time-Domain buffer of user type $i \in \{c, v\}$	D_i	Average packet delay of user type $i \in \{c, v\}$
ϵ	Channel Correlation Coefficient	r_0	Minimum rate requirement of CUEs
P_i^c	Transmit power of user type $i \in \{c, v\}$	p_0	Maximum Outage probability of VUEs
P_{max}^c	Maximum transmit power of CUEs	γ_0	Minimum SINR Threshold for VUEs
P_{max}^v	Maximum transmit power of VUEs	C_t	maximum number of users scheduled per TTI
N_v	Number of RBs required by a VUE v	N_c	Number of RBs required by CUE c

CSI for power control. Authors in [25] propose a one-to-many matching resource sharing problem where one V2V pair can share the RBs assigned to multiples V2I users. In [26] is proposed an unsupervised learning-based power control technique that maximizes the sum capacity of V2I and V2V users. Data-driven methods are used in [27, 28] for resource allocation and V2V user grouping with partial-CSI in C-V2X networks. The work in [29] addresses the problem of heterogeneous QoS provisioning through joint power and spectrum allocation while trying to maximize the number of V2V pairs. It assumes that the global CSI information is unavailable.

In contrast to existing works, in this article, we have not only considered resource sharing and power allocation but have also incorporated the link-adapted resource allocation of V2I users to maximize the V2I user capacity as well as their sum capacity, while supporting the stringent delay and QoS requirements of both V2I and V2V users.

III. SYSTEM MODEL

Fig. 1 shows an overview of the system model, developed according to [5], and is explained in this section along with the problem formulation. Table II outlines the symbol definitions.

A. System Model

1) **Scenario and User Distribution:** In this work, we have considered the service area of a single gNB, in which the gNB is located at the center as shown in Fig. 1. We have assumed that there are N_L lanes inside this area, each of width w metres, located to the south of the gNB. There are C stationary V2I users or Cellular User Equipments (CUEs), V V2V pairs or Vehicular UEs (VUEs), and M stationary Best-Effort UEs (BUEs). The CUEs and BUEs are uniformly distributed in the service area, excluding the lanes. All the VUEs have the same velocity ν and have been dropped uniformly in the lanes [37]. We have shown in Fig.1 only a few CUE, BUEs, and VUE pairs and four lanes to maintain clarity.

2) **User Traffic and Packet Generation:** The CUEs and BUEs communicate directly with the gNB. We have assumed that the network traffic generated by the CUEs is mostly of infotainment nature, such as voice or video calling, multimedia streaming, etc. These users, thus, have a rate constraint and a delay constraint. The transmitter and the receiver of the VUE pairs communicate only amongst themselves and primarily

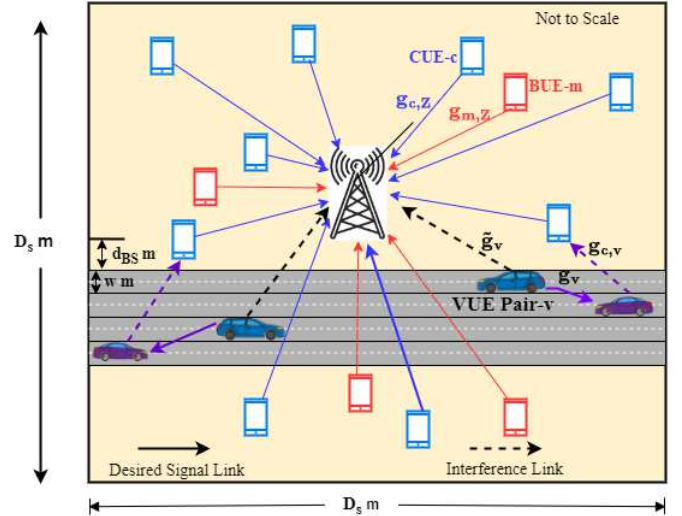


Figure 1: A simplified version of the System Model. Only a few CUEs, BUEs, VUE pairs, and four lanes have been shown in the general NodeB (gNB) service area.

Table III: Different Numerologies in 5G NR

Numerology Index	Sub-Carrier Spacing $\Delta f = 2^\mu \times 15\text{KHz}$	Bandwidth of one RB (KHz)	TTI duration (ms)
0	15	180	1
1	30	360	0.5
2	60	720	0.25
3	120	1440	0.125
4	240	2880	0.0625

exchange safety enhancement messages. So, they have a coverage probability constraint, and their delay constraint is more stringent than the CUEs. Thus, the CUEs and VUEs generate delay-sensitive real-time traffic. While a CUE generates a packet of β_c bytes every τ_c ms, a VUE generates a packet of β_v bytes every τ_v ms. The number of CUEs generating a packet in a time slot follows a Poisson distribution with a mean $\lambda_c = \frac{\text{Total no. of CUEs}}{20\text{ms}}$. The delay constraint or time-to-live for the CUE and VUE packets is δ_c ms and δ_v ms, respectively. The BUEs essentially communicate non-real-time traffic with no QoS requirement. Their traffic is of full buffer type, *i.e.* they always have some data to send.

3) **Multiple Numerologies and OFDMA:** To support the diverse QoS requirements as mentioned in Section III-A2, we have used the multiple numerology frame structure of 5G

NR [5]. We have divided the system bandwidth into two bandwidth parts (BWPs), each supporting different numerologies. As 5G uses OFDMA, each BWP is divided into orthogonal time-frequency radio RBs spanning 12 Orthogonal Frequency Division Multiplexing (OFDM) sub-carriers in the frequency domain and 14 OFDM symbols in the time domain. So, the bandwidth of a RB is $12 \times \text{Sub-carrier Spacing (SCS)}$, and the duration of 14 symbols constitutes one Transmission Time Interval (TTI). The different numerologies are characterized by different SCSs and different TTI durations, as specified in Table III. Users of different applications are assigned different numerologies, *i.e.*, to different BWPs based on their QoS requirements. For example, the numerology in BWP-1 is $\mu = 3$ with a SCS of 120 KHz and a TTI duration of 0.125 milliseconds (ms). It caters to time-critical applications, such as the CUEs and VUEs. On the other hand, BWP-2 of bandwidth B_2 has a numerology $\mu = 0$ with a SCS of 15 KHz and a slot duration of 1 ms, and it serves the BUEs.

To minimize the interference among the neighbouring CUEs, the gNB allocates orthogonal uplink RBs from BWP-1 to the CUEs. ρ_c^n represents the allocation variable, such that $\rho_c^n = 1$, if RB n is allocated to CUE c , and $\rho_c^n = 0$, otherwise.

4) **Modes of RB Allocation:** We explore two modes of RB allocation between the CUEs and VUEs [11] –

- (i) **Shared or Underlay mode** - in which the VUEs operate in the D2D side link, *i.e.*, the uplink resources of CUEs are reused by the VUEs. This is made possible because of the small amount of interference that VUEs generates to the uplink communication between the CUEs and the gNB. Power control can minimize this interference, as explained in Section IV-A2a. We set the indicator variable $x_{c,v} = 1$ if the RBs of CUE c are shared with VUE v , otherwise we set, $x_{c,v} = 0$, $\forall c \in \mathcal{C} = \{1, 2, \dots, C\}$, and $\forall v \in \mathcal{V} = \{1, 2, \dots, V\}$.

- (ii) **Dedicated or Overlay Mode** - in which the CUEs and the VUEs are assigned orthogonal RBs.

5) **Channel Modeling:** The next important step is channel modeling. We assume that the small-scale fast-fading gain h_v^n of the VUE v in RB- n , is independent and identically distributed (i.i.d) as $\mathcal{CN}(0, 1)$ for all VUEs. We further assume a block fading channel model in which h_v^n for VUE v is different in different RBs in the same TTI. The corresponding channel gain g_v^n of the VUE pair v in RB- n is given by,

$$g_v^n = |h_v^n|^2 \alpha_v, \quad (1)$$

where α_v is the large-scale fading gain. Applying the assumptions mentioned above to the different communication links in Fig. 1, the respective channel gains can be defined as:

- 1) $g_{c,Z}^n$ - Uplink channel gain in RB- n between a CUE c and the gNB Z ,
- 2) $g_{m,Z}^n$ - Uplink channel gain in RB- n between a BUE m and the gNB Z ,
- 3) g_v^n - channel gain of a VUE pair over RB- n ,
- 4) \tilde{g}_v^n - Interference from VUE pair v to the CUE-gNB communication over RB- n ,
- 5) $\tilde{g}_{c,v}^n$ - Interference from the CUE c to the VUE v in RB- n .

Large-scale fading, composed of path loss and shadowing, depends only on the user positions and varies slowly. Hence,

they are perfectly determined at the gNB for all links. It is also assumed that the channel gains, $g_{c,Z}^n$, $g_{m,Z}^n$ and \tilde{g}_v^n , of links directly connected to the gNB can be accurately obtained at the gNB. However, the channel gains, g_v^n and $\tilde{g}_{c,v}^n$, of links that are not directly connected to the gNB are reported with a feedback period of one TTI, of duration T . The high mobility of vehicles also introduces the Doppler shift in the small-scale fading. We, thus, assume that the gNB can only obtain the estimated channel fading h with an error e . The gain h follows a first-order Gauss-Markov process over a period T , *i.e.*,

$$h = \hat{e}h + e, \quad (2)$$

where h and \hat{h} represent the small-scale fading gain in the current and previous TTIs, respectively. The channel difference, e , between two consecutive TTIs, follows an i.i.d $\mathcal{CN}(0, 1 - \epsilon^2)$ distribution. It is independent of \hat{h} . The channel correlation coefficient ϵ between two consecutive TTIs follows Jake's fading model [38], such that $\epsilon = J_0(2\pi f_d T)$. Here $J_0(\cdot)$ is the zeroth-order Bessel function of the first kind, $f_d = \nu f_c / c$ is the maximum Doppler shift in frequency with $c = 3 \times 10^8$ m/s, ν is the vehicular speed, and f_c is the carrier frequency.

The SINR of the CUE c in the RB- n in shared mode is,

$$\gamma_c^n = \frac{P_c^C \alpha_{c,Z} |h_{c,Z}^n|^2}{\sigma^2 + \sum_{v=1}^V x_{c,v} P_v^V \tilde{\alpha}_v |\tilde{h}_v^n|^2}, \quad (3)$$

and the SINR of the VUE v is.

$$\gamma_v^n = \frac{P_v^V \alpha_v (\epsilon_v^2 |\hat{h}_v^n|^2 + |e_v^n|^2)}{\sigma^2 + \sum_{c=1}^C x_{c,v} P_c^C (\epsilon_{c,v}^2 |\hat{h}_{c,v}^n|^2 + |e_{c,v}^n|^2)}, \quad (4)$$

where P_c^C and P_v^V are the transmit powers of CUE c and VUE v , respectively. σ^2 is the noise power. We assume a packet is served within one TTI without any retransmission.

6) **Link Adaptation:** Finally, we discuss link adaptation, which is used in this work to tune the number of RBs required by a packet to the underlying channel conditions. This is in contrast to existing works that implement CUE packet transmission using a single RB only. The number of RBs required to transmit a packet in a TTI is calculated as $\frac{\text{Packet size in bits}}{\text{Num of bits/RB}}$, where $\text{Num of bits/RB} = \text{num of symbols/RB} \times \text{num of bits/symbol}$. The number of symbols per RB depends on the number of sub-carriers in a RB and the number of symbols in a TTI. So, from Section III-A3, the number of symbols per RB is 12×14 , and the number of bits per RB is $12 \times 14 \times \text{number of bits/symbol}$. The number of bits per symbol, *i.e.*, the user's spectral efficiency (SE), on the other hand, depends on the MCS, which in turn depends on the user's SINR and BLER requirement. Table IV [1, Table 3] shows the different MCSs, the corresponding SE and SINR ranges for different BLERs. It may be observed that for a given BLER, a higher SINR supports a higher MCS, and, hence, a higher SE. However, for the same SINR, a lower BLER implies a lower MCS needs to be selected. Table IV also shows the number of RBs needed to serve a CUE or a VUE packet. So, once the SINR of the CUE (or VUE) is obtained, its MCS and, hence, its SE for a given BLER is obtained from Table IV. Subsequently, the number of RBs required is also calculated according to the packet size.

Table IV: Modulation and Coding Schemes, Spectral Efficiency, and Signal-to-Noise Ratio ranges to support different BLERs

MCS	1	2	3	4	5	6	7	8	9	10	11	12	13	14	15
Modulation	QPSK	QPSK	QPSK	QPSK	QPSK	QPSK	16 QAM	16 QAM	16 QAM	64 QAM	64 QAM	64 QAM	64 QAM	64 QAM	64 QAM
Spectral Efficiency (bits/symbol)	0.15	0.23	0.38	0.6	0.88	1.18	1.48	1.91	2.41	2.73	3.32	3.90	4.52	5.12	5.55
SNR Th (dB) BLER _c = 0.1	-6.5	-4.0	-2.6	-1	1	3	6.6	10.0	11.4	11.8	13.0	13.8	15.6	16.8	17.6
SNR Th (dB) BLER _v = 0.01	-2.5	0.0	1.4	3.0	5.0	7.0	10.6	14.0	15.4	15.8	17.0	17.8	19.6	20.8	21.6
No. of RBs required for a 50 byte packet	16	11	7	4	3	3	2	2	1	1	1	1	1	1	1
No. of RBs required for a 10 byte packet	4	3	2	1	1	1	1	1	1	1	1	1	1	1	1

B. Problem Formulation for Shared mode

This section explains the problem formulation for the shared resource allocation mode. We aim to find a) the optimal resource allocation of CUEs, and 2) the optimal pairing between CUEs-VUEs such that the sum rate of the CUEs is maximized. At the same time, the delay and rate constraints of CUEs and the delay and coverage probability constraints of VUEs should be satisfied. We denote the transmission rate of CUE- c in RB- n is R_c^n , which can be obtained from Table IV. So, the optimization problem is:

$$\max_{\{\rho_c^n\}, \{x_{c,v}\}, \{P_v^V\}, \{P_c^C\}} \sum_n \sum_{c \in \mathcal{C}} R_c^n \rho_c^n \quad (5)$$

s.t.

$$\sum_{c \in \mathcal{C}} \rho_c^n \leq 1, \forall n, \quad (6a)$$

$$D_c \leq \delta_c, \forall c \in \mathcal{C}; D_v \leq \delta_v, \forall v \in \mathcal{V} \quad (6b)$$

$$\sum_n R_c^n \rho_c^n \geq r_0, \forall c \in \mathcal{C} \quad (6c)$$

$$\Pr\left\{\sum_n \gamma_v^n \rho_n^c x_{c,v} \leq \gamma_0\right\} \leq p_0, \forall v \in \mathcal{V} \quad (6d)$$

$$0 \leq P_c^C \leq P_{\max}^C, \forall c \in \mathcal{C} \quad (6e)$$

$$0 \leq P_v^V \leq P_{\max}^V, \forall v \in \mathcal{V} \quad (6f)$$

$$\sum_{c \in \mathcal{C}} x_{c,v} \leq 1, x_{c,v} \in \{0, 1\}, \forall v \in \mathcal{V} \quad (6g)$$

$$\sum_{v \in \mathcal{V}} x_{c,v} \leq 1, x_{c,v} \in \{0, 1\}, \forall c \in \mathcal{C}. \quad (6h)$$

The details of the constraints are as follows.

- **RB allocation constraint** - (6a) says that (i) one RB can be assigned to only one CUE. The total number of RBs occupied by the CUEs should be less than or equal to N_1 , i.e., the number of RBs in BWP-1.
- **Delay constraint** - (6b) says that the average packet delays, D_c and D_v of a CUE and VUE should be less than their time-to-live δ_c and δ_v , respectively.
- **Minimum Rate constraint** - (6c) says that RBs are shared between CUE and VUE if the minimum required rate r_0 of CUEs is guaranteed.

- **Coverage Probability constraint** - (6d) says that the resource sharing between CUEs and VUEs should ensure the coverage of VUEs. Here, γ_0 is the minimum SINR required for a reliable VUE communication, and p_0 is its maximum outage probability.
- **Power Allocation Constraint** - (6e) and (6f) give the range of transmit powers of the CUEs and VUEs, respectively, upper bounded by P_{\max}^C and P_{\max}^V .
- **Resource Sharing Constraint** - (6g) and (6h) ensure that the RBs of only one CUE is shared with only one VUE.

IV. PROPOSED POWER AND SPECTRUM ALLOCATION WITH LINK ADAPTATION

This section discusses the proposed resource allocation algorithms for the modes mentioned in Section III-A4, i.e., 1) shared or underlay, and 2) dedicated or overlay.

A. Greedy Resource Allocation Hungarian Sharing

The first proposed algorithm, **Greedy Resource Allocation with Hungarian Sharing (GRAHS)**, which is outlined as Algorithm 1 works as follows. (i) First, it executes a greedy approach to allocate resources to the CUEs according to their link condition (Section IV-A1). (ii) Using this resource allocation, it allocates power to the CUEs and VUEs (Section IV-A2a). (iii) With the new power allocation from step (ii), GRAHS pairs the CUEs and VUEs, using the maximum weighted bipartite matching Hungarian algorithm, such that each CUE-VUE pair meets the CUE rate constraint and the VUE coverage probability constraint. (iv) Finally, GRAHS checks all the paired CUEs and VUEs to ascertain if the number of RBs required by the corresponding CUE after pairing conforms to its respective QoS requirement or not. If not, it declares the pairing infeasible. The details follow.

1) **Resource Allocation of CUEs** : GRAHS runs at the beginning of every TTI. CUEs and VUEs being real-time traffic users, their packets have expiry deadlines. So, GRAHS starts by sorting the CUE and VUE packets independently into two different buffers, \mathcal{B}_C and \mathcal{B}_V , respectively, according to their time-to-live. This sends the earliest packet to the head of the queue, addressing the delay sensitivity. It then allocates

Algorithm 1: Proposed GRAHS

```

1 for  $t \in \{1, 2, \dots, T_{\text{obs}}\}$  do
2   Sort CUE and VUE packets into the buffers  $\mathcal{B}_C$ 
   and  $\mathcal{B}_V$  according to their time-to-live.;
3   for  $c \in \mathcal{B}_C$  do
4     if No. of CUEs scheduled  $\leq C_t$  then
5       Find channel gain  $g_{c,Z}^n = |h_{c,Z}^n|^2$  between
       the  $c^{\text{th}}$  CUE and gNB in RB- $n$ ,  $\forall n$ ;
6       Calculate SNR  $\gamma_c^n = \frac{P_c^C \alpha_{c,Z} |h_{c,Z}^n|^2}{\sigma^2}$  in each
       RB and obtain the SE  $R_c^n$  from Table IV
       for a BLER of 0.1.;
7       Sort all  $N_1$  RBs in BWP-1 in descending
       order of  $R_c^n$ ;
8       Find the greedy resource allocation ( $\rho_c^n$ )
       that maximizes  $R_c' = \sum_{n=1}^{N_1} R_c^n \rho_c^n$  using
       minimum possible number of RBs,  $N_c$ ;
9       Add  $c$  to the scheduled CUE list  $\mathcal{S}_C$ ;
10      for  $v \in \mathcal{B}_V$  do
11        For the pair  $\{c, v\}$  obtain the optimal
        power allocation  $P_v^*, P_c^*$  from (9) and
        (10) [24];
12        Obtain  $R_c^*$  by substituting  $P_c^*, P_v^*$ ;
13        if  $R_c^* < r_0$  &&
         $\Pr\{\sum_n \gamma_v^n \rho_n^c x_{c,v} \leq \gamma_0\} > p_0$  then
14           $R_c^* = -\text{inf}$ ;
15      Use Hungarian algorithm to find optimal pairing
       $x_{c,v}$  between CUEs and VUEs based on  $R_c^*$ ;
16      for  $c \in \mathcal{S}_C$  do
17        for  $v \in \mathcal{B}_V$  do
18          if  $x_{c,v} == 1$  then
19            Calculate the SE per RB,  $R_c^n$  and  $R_v^n$ 
            using the SINR  $\gamma_c^n$  and  $\gamma_v^n$  from (3)
            and (4), respectively;
20            Calculate the number of RBs  $N_c^*$  and
             $N_v^*$  using  $R_c^n$  and  $R_v^n$ ;
21            if  $N_c^* = N_c$  &  $N_v^* \leq N_c$  then
22              Assign RBs with  $\rho_c^n = 1$  to VUE  $v$ ;
23            else
24              Scheduling the VUE in next TTI;
25      return The RB allocation  $\rho_c^{n*}$  of CUEs, the
      optimal pairing  $x_{c,v}$  between CUEs and VUEs,
      and the optimal power allocation  $P_c^*, P_v^*$ ;
    
```

RBs to the CUEs only. First, GRAHS determines the channel gain $g_{c,Z}^n$ (Line 5) and calculates the Signal-to-Noise-Ratio (SNR) of CUE c in RB- n as $\gamma_c^n = \frac{P_c^C g_{c,Z}^n}{\sigma^2}$, $\forall n$ (Line 6). At this point, GRAHS considers that a RB is not yet shared with a VUE. So, the SNR, and not SINR, of the CUEs, is computed. For the SNR computed in Line - 6, GRAHS then uses Table IV to find out the MCS and the transmission rate R_c^n that it can use to serve the CUE packet with a BLER of 0.1. It uses this MCS value to find the required number of RBs, N_c .

GRAHS then finds the greedy resource allocation in Line-8. To explain the greedy resource allocation, we use the example in Table V. Each row in the table represents a CUE and its

Table V: An example of achievable Spectral Efficiency of different users in different RBs.

CUE Id	SE in each RB (bits/symbol)/ No. of bits per RB				
	RB ₁	RB ₂	RB ₃	RB ₄	RB ₅
c_1	1.18/198.24	1.18/198.24	1.48/248.64	1.48/248.64	1.91/320.88
c_2	1.91/320.88	1.91/320.88	1.91/320.88	1.48/248.64	1.48/248.64
c_3	1.48/248.64	1.48/248.64	1.48/248.64	1.48/248.64	1.18/198.24

channel condition in the different RBs. Each cell in Table V, under the columns labeled RB _{i} , has an x/y element, where ‘ x ’ is the user’s SE in bits/symbol and ‘ y ’ is the number of bits per RB, for the SE x . The CUEs in the leftmost column are sorted in the order of their shortest time-to-live., i.e., $c_1 < c_2 < c_3$. For each CUE, we first sort the RBs in the descending order of achievable SEs. So, the sorted list for c_1 is RB₅, RB₃, RB₄, RB₁, RB₂. The algorithm scans this sorted list and checks if the RB with the highest SE can accommodate the packet. This example shows that RB₅ has the highest SE of 1.91 bits/symbol for c_1 . To serve a 50-byte packet with this SE, two RBs will be needed. However, no other RB has the same or higher SE. Hence, the algorithm moves to the RB with the second-highest SE, which here is RB₃. Its SE is 1.48 bits/symbol. It is found that for this SE also, two RBs are needed to accommodate a CUEs’s packet. So, GRAHS assigns RB₅, which has a higher SE than RB₃, and RB₃ to c_1 . In this case, the SE used in both RBs is that of RB₃, as RB₃ will not be able to handle a higher SE. Subsequently, these RBs become unavailable to other CUEs. If, however, the packet could not be accommodated within the two RBs, the search would have continued to identify three, four, or more RBs in which the packet could be served, albeit with a lower MCS, according to Table IV¹. In this way, GRAHS accommodates a CUE packet using minimum number of RBs based on the first fit strategy to achieve a lower complexity. In such a multiple RB assignment, the minimum achievable SE among all assigned RBs is used. This is because a RB which has a higher SNR can support the lower SE, but the reverse is not true [35].

This part of the algorithm returns the RB allocation variable $\rho_c^n, \forall n$, of the CUEs. The CUEs which are allocated RBs in Line-8, are added to the scheduled list \mathcal{S}_C in Line-9. An important point to note is that the maximum number of users that can be scheduled in a TTI is limited by the availability of the Physical Uplink Control Channel (PUCCH) [39]. So, we have assumed that the number of users that can be scheduled at a time is limited by C_t , (Line-4). The algorithm next pairs the CUEs and VUEs for RB sharing.

2) **Resource Sharing between CUEs and VUEs:** : The resource sharing between CUEs and VUEs includes: a) the power allocation to the CUE-VUE pairs so that the interference is limited (Line - 11), and b) selection of the optimal CUE-VUE pairs (Line - 15).

a) **Optimal Power Allocation:** After RB allocation, GRAHS allocates power to all the CUE-VUE pairs in the RBs assigned to the CUEs [24]. In other words, for the CUE-

¹It may be noted that the explanation above also holds for RB₅ and RB₄, instead of RB₅ and RB₃ as RB₄ and RB₃ have the same SE.

c , GRAHS allocates power to all the V VUE connections in the RBs assigned to c , i.e., those with $\rho_c^n = 1$. The power is allocated in a way that maximizes the CUE rate while satisfying the coverage probability constraint of VUEs in (6d) [24]. As mentioned earlier, after RB allocation, the minimum achievable transmission rate among all the RBs assigned to a CUE is used in each RB. So, the objective of the power allocation is to maximize this minimum transmission rate. We denote the minimum transmission rate as $R_{c,\eta}$

$$R_{c,\eta} = B \log_2 \left(1 + \frac{P_c^C \alpha_{c,z} |h_{c,z}^\eta|^2}{\sigma^2 + P_v^V \alpha_v |h_v^\eta|^2} \right), \quad (7)$$

where $\eta = \underset{n}{\operatorname{argmin}}(R_c^n), \forall n$ with $\rho_c^n = 1$. Thus, the problem can be rewritten in this part as:

$$(P_c^*, P_v^*) = \underset{P_c^C, P_v^V}{\operatorname{argmax}} R_{c,\eta} \quad (8)$$

s. t. (6d), (6e) and (6f) are satisfied.

The optimal power allocation from (8) is:

$$P_v^* = \begin{cases} \min\{P_{\max}^V, P_{\mathcal{C},\max}^{V_1}\}, & \text{if } P_{\max}^V \leq P_0^V, \\ \min\{P_{\max}^V, P_{\mathcal{C},\max}^{V_2}\}, & \text{if } P_{\max}^V > P_0^V, \text{ and } P_{\max}^C > P_0^C, \\ P_{\mathcal{C},\max}^{V_1}, & \text{otherwise,} \end{cases} \quad (9)$$

and

$$P_c^* = \begin{cases} \min\{P_{\max}^C, P_{\mathcal{V},\max}^{C_1}\}, & \text{if } P_{\max}^V \leq P_0^V, \\ \min\{P_{\max}^C, P_{\mathcal{V},\max}^{C_2}\}, & \text{if } P_{\max}^V > P_0^V, \text{ and } P_{\max}^C > P_0^C, \\ P_{\max}^C, & \text{otherwise,} \end{cases} \quad (10)$$

where

$$P_0^C = \frac{\sigma^2}{\frac{1-\epsilon_{c,v}^2}{1-\epsilon_v^2} \left(\frac{1}{p_0} - 1 \right) \alpha_{c,v} \epsilon_v^2 |\hat{h}_v^\eta|^2 - \alpha_{c,v} \epsilon_{c,v}^2 |\hat{h}_{c,v}^\eta|^2} \quad (11)$$

and

$$P_0^V = \frac{P_0^C \gamma_0 \alpha_{c,v} (1 - \epsilon_{c,v}^2) (1 - p_0)}{\alpha_v (1 - \epsilon_v^2) p_0} \quad (12)$$

$P_{\mathcal{C},\max}^{V_1}$ and $P_{\mathcal{V},\max}^{C_1}$ are derived from the functions,

$$\mathcal{F}_1(P_{\mathcal{C},\max}^{V_1}, P_{\max}^C) = 0 \text{ and } \mathcal{F}_1(P_{\max}^V, P_{\mathcal{V},\max}^{C_1}) = 0. \quad (13)$$

$P_{\mathcal{C},\max}^{V_2}$ and $P_{\mathcal{V},\max}^{C_2}$ are derived from the functions,

$$\mathcal{F}_2(P_{\mathcal{C},\max}^{V_2}, P_{\max}^C) = 0 \text{ and } \mathcal{F}_2(P_{\max}^V, P_{\mathcal{V},\max}^{C_2}) = 0. \quad (14)$$

through bisection search by noting the monotonic relation between P_c^C, P_m^V in the functions,

$$\mathcal{F}_1(P_c^C, P_v^V) = \exp\left(\frac{G\gamma_0}{F}\right) \left(1 + \frac{H}{F}\gamma_0\right) - \frac{\exp\left(\frac{A}{F}\right)}{1-p_0} = 0$$

when $P_v^V \in (0, P_0^V)$ and

$$\mathcal{F}_2(P_c^C, P_v^V) = \left(1 + \frac{F}{\gamma_0 H}\right) \exp\left(\frac{A - G\gamma_0}{\gamma_0 H}\right) - \frac{1}{p_0} = 0$$

when $P_v^V \in (P_0^V, +\infty)$. Here, $A = P_v^V \alpha_v \epsilon_v^2 |\hat{h}_v^\eta|^2$, $F = P_v^V \alpha_v (1 - \epsilon_v^2)$, $G = \sigma^2 + P_c^C \alpha_{c,v} \epsilon_{c,v}^2 |\hat{h}_{c,v}^\eta|^2$ and $H = P_c^C \alpha_{c,v} (1 - \epsilon_{c,v}^2)$.

b) Hungarian algorithm for Resource Sharing (HS):

With the new power allocation (P_c^*, P_v^*) , the minimum transmission rate of the RBs assigned to a CUE is recalculated as $R_{c,\eta}^* = B \log_2 \left(1 + \frac{P_c^* \alpha_{c,z} |h_{c,z}^\eta|^2}{\sigma^2 + P_v^* \alpha_v |h_v^\eta|^2} \right)$. Consequently, GRAHS obtains the new CUE rate $\hat{R}_c^* = R_{c,\eta}^* \sum_n \rho_c^n$ (Line 12). The VUEs for which R_c^* meets the rate constraint of (6c) and which meet the coverage probability constraint of (6d) are added to the candidate VUE list for resource sharing with CUE c . After all the CUEs and VUEs are scanned, they need to be paired in such a way that maximizes the transmission rate of the CUEs. This pairing problem is one of maximum weighted bipartite matching in which the two sets are the CUEs and the VUEs. The weights of the links between these sets are the transmission rates of the CUEs. The maximum weight perfect matching of these sets can be obtained in polynomial time using the Hungarian algorithm [24, 32], which we have done in this work. This step returns the pairing variable $x_{c,v}, \forall c, \forall v$.

3) **Final Allocation:** At this stage, GRAHS has the RB allocation of the CUE- c stored in ρ_c^n and the pairing of the CUE- c and VUE- v stored in $x_{c,v}$. It next checks whether the pairs are viable with respect to their RB requirement.

GRAHS picks each $\{c, v\}$ pair with $x_{c,v} = 1$ and recalculates the SINRs γ_c^n and γ_v^n from (3) and (4), respectively, in the RBs which are assigned to CUE- c only (i.e., the RBs with $\rho_c^n = 1$). Thus, at this point, the algorithm accounts for the interference between the CUEs and VUEs. It then uses Table IV to calculate the number of RBs, N_c^* , needed to serve a CUE packet with a BLER of 0.1 using the newly calculated SINR γ_c^n (3). Similarly, it also estimates N_v^* , i.e., the number of RBs needed to serve a VUE packet with a BLER of 0.001 using the newly calculated SINR γ_v^n (4). To find N_c^* and N_v^* , it uses the same method as explained in Section III-A6. The CUE-VUE pair (c, v) is finalized if and only if $N_c^* = N_c$ and $N_v^* \leq N_v$. Otherwise, the algorithm assigns resources to the CUE only and defers the allocation of the VUE till the next slot. This step returns the updated sharing variable $x_{c,v}^*$.

B. Hungarian Resource Allocation Hungarian Sharing

A major drawback of GRAHS is that it does not allocate contiguous RBs to the users. However, 3GPP advocates contiguous resource block allocation, especially in the Frequency Range 2 [40–42]. So, we have designed a second resource allocation algorithm for the CUEs, in which instead of treating each RB independently, we have grouped a few RBs into one Resource Chunk (RC) [33, 34]. The algorithm assigns one RC to one CUE in each TTI such that the sum rate of the CUEs is maximized. Thus, this assignment problem of the CUEs to RCs is also one of maximum weight bipartite matching, in which the sets to be matched are the CUEs and the RCs, and the weights are the rates of the CUE. So, we have used the Hungarian algorithm for assigning RCs to CUEs. Therefore, the second algorithm of our work uses the Hungarian assignment in two stages - first to assign RCs to the CUEs, and then to pair the CUEs with the VUEs. We call this algorithm **HRAHS** - Hungarian Resource Allocation with Hungarian Sharing, which is outlined as Algorithm 2.

We have observed from extensive simulations of GRAHS

Algorithm 2: Proposed HRAHS

```

1 for  $t \in \{1, 2, \dots, T\}$  do
2   Sort CUE and VUE packets into the buffers  $\mathcal{B}_C$ 
   and  $\mathcal{B}_V$  according to their time-to-live.;
3   if  $\text{len}(\mathcal{B}_C) < C_t$  then
4     Append  $\{C_t - \text{len}(\mathcal{B}_C)\}$  null users to  $\mathcal{B}_C$ ;
5   for  $c \in \mathcal{B}_C[1 : C_t]$  do
6     Find the CSI  $g_{c,Z}^j$  in RC- $j$ ,  $\forall j$  RCs, between
     the  $c^{\text{th}}$  CUE and the gNB;
7     Using  $g_{c,Z}^j$ , calculate the rate
      $R_c^j = \log_2(1 + \frac{P_c^c \alpha_{c,Z} |h_{c,Z}^j|^2}{\sigma^2})$  in each RC.;
8   Use a maximizing Hungarian algorithm to find the
   optimal pairing between  $C_t$  CUEs of  $\mathcal{B}_C$  and the
    $C_t$  RCs so as to maximize  $\sum_j \sum_c R_c^j$ . while
   providing a BLER=0.1;
9   Add scheduled CUEs to the list  $\mathcal{S}_C$ ;
10  for  $c \in \mathcal{S}_C$  do
11    for  $v \in \mathcal{V} = \{1, 2, \dots, V\}$  do
12      For the pair  $\{c, v\}$  obtain the optimal power
      allocation  $P_v^*, P_c^*$  from (9) and (10) [24];
13      Obtain  $R_c^*$  by substituting  $P_c^*, P_v^*$ ;
14      if  $R_c^* < r_0$  then
15         $R_c^* = -\text{inf}$ ;
16    Use Hungarian algorithm to find optimal pairing
     $x_{c,v}$  between CUEs and VUEs based on  $R_c^*$ ;
17    for  $c \in \mathcal{S}_C$  do
18      for  $v \in \mathcal{B}_v$  do
19        if  $x_{c,v} == 1$  then
20          Calculate the SE per RB,  $R_c^n$  and  $R_v^n$ ,
          for the RBs of the RC allocated to
          CUE  $c$  ( $\zeta_c^j = 1$ ) using the SINR  $\gamma_c^n$ 
          and  $\gamma_v^n$  from (3) and (4), respectively;
21          Calculate the number of RBs  $N_v^*$  using
           $R_c^n$  and  $R_v^n$  for BLER = 0.001;
22          if  $N_v^* \leq \text{size}(\text{RC})$  then
23            Assign  $N_v^*$  RBs, from the RC
            allocated to CUE  $c$ , to the VUE  $v$ ;
24          else
25            Scheduling of VUE is deferred to
            the next slot;
26  return The optimal RC allocation  $\zeta_c^{j*}$  of CUEs,
  the optimal pairing  $x_{c,v}^*$  between CUEs and
  VUEs, the optimal power allocation  $P_c^*, P_v^*$ , and
  the RB allocation of VUEs;

```

(10 simulation runs, each of 6.25 seconds) that on an average 2.14, *i.e.*, three RBs are required to serve a packet of size 50 bytes for a BLER of 0.1. Furthermore, we have also observed that nearly 92.78% of users needed fewer than four RBs. Hence, we have grouped four RBs to form a RC. It is to be noted that the size of the RCs is a design choice and may be changed based on the network scenario.

HRAHS runs at the beginning of a TTI and sorts the CUE and VUE packets according to their time-to-live. into the two independent buffers, \mathcal{B}_C and \mathcal{B}_V , respectively. Once

the packets are sorted, it first allocates resources to the CUEs without considering any interference from the VUEs. We represent the SNR (SINR) of CUE c in RC j as γ_c^j (γ_c^j). We introduce a new RC allocation variable ζ_c^j , such that $\zeta_c^j = 1$, if CUE c is allocated to RC j , and $\zeta_c^j = 0$, otherwise, $\forall c \in \mathcal{C}$ and $\forall j \in \mathcal{J}$. Here, \mathcal{J} gives the set of all RCs. We assume, the number of RCs in \mathcal{J} is equal to the maximum number of users that can be scheduled in a TTI, which here is C_t . Thus, the resource allocation problem of CUEs reduce to:

$$\max_{\{\zeta_c^j\}} \sum_{j \in \mathcal{J}} \sum_{c \in \mathcal{C}} R_c^j = \log_2(1 + \gamma_c^{j'}). \quad (15)$$

(15) is, thus, a $C_t \times C_t$ maximum weight bipartite matching problem, which matches C_t users to C_t RCs with the objective of maximizing R_c . In some TTIs, however, the number of CUEs in the buffer \mathcal{B}_C can be less or more than C_t . If it is less than C_t , then HRAHS first appends $C_t - |\mathcal{B}_C|$ null users to \mathcal{B}_C (Line-3 Algorithm 2) in order to execute the Hungarian algorithm. Otherwise, it selects the first C_t users for allocation to the RCs (Line-5 Algorithm 2).

HRAHS next allocates power to each CUE-VUE pair in the RCs (Line-12) so as to maximize the CUE datarate, as in GRAHS. It then recalculates the CUE rate R_c^* with the new power allocation, and uses R_c^* to pair the CUEs and VUEs for sharing the RCs, using Hungarian algorithm (Line-16 for Algorithm 2). The pairing using Hungarian algorithm ensures that the CUE rate is maximized while satisfying both the CUE rate constraint and the VUE coverage probability constraints, generating the pairing variable $x_{c,v}$.

Once the pairing is done, the algorithm then selects each $\{c, v\}$ pair and recalculates the SINR, γ_c^n and γ_v^n , in all the RBs of the RC assigned to CUE c , (*i.e.*, the RBs in the RC having $\zeta_c^j = 1$). It then uses γ_v^n to calculate the number of RBs, N_v^* , needed to transmit a VUE packet at a BLER = 0.001. If N_v^* is less than or equal to the size of a RC, the CUE c and VUE v are paired. Otherwise, the VUE v is scheduled in the next TTI. If N_v^* is less than the size of a RC, then N_v^* RBs from the RC allocated to CUE c are assigned to the VUE v . This method returns the optimal RC allocation ζ_c^{j*} , the optimal pairing $x_{c,v}^*$, and the optimal power allocation P_c^*, P_v^* .

C. Overlay Resource Allocation (ORA)

To establish the performance of GRAHS and HRAHS, we have compared them to the dedicated or the Overlay mode of Resource Allocation – ORA. In ORA, CUEs and VUEs do not share resources. Instead, VUEs are also assigned dedicated RBs. So, CUEs and VUEs packets are first sorted into a single array according to their time-to-live.. Then, their SNRs (no resource sharing, hence, no interference) are obtained in all the RBs, and the number of RBs needed to serve a CUE and a VUE packet is calculated as in Section III-A6. Finally, similar to GRAHS, a greedy resource allocation approach is adopted to assign the RBs to the users. As VUEs are also assigned dedicated RBs, hence the limit on the number of users that can be scheduled in a TTI applies to both CUEs and VUEs.

D. Resource Allocation of Best Effort Users

For the resource allocation algorithms - GRAHS (Section IV-A), HRAHS (Section IV-B), ORA (Section IV-C)- a separate BWP is reserved for the BUEs. This BWP-2, as mentioned in Section III-A, has a SCS of 15 KHz and a time slot of 1 ms. So, the bandwidth of each RB is 180 KHz. These RBs are allocated to the BUEs using Max C/I algorithm [43]. In a TTI, we assign each RB to that BUE which has the highest CSI in that RB. The resultant scheme is not fair, but it maximizes the sum rate of the BUEs.

E. Complexity Analysis

We next compare the algorithms in terms of their time complexity.

For each CUE, GRAHS executes the following steps.

- 1) It sorts the RBs according to the SEs achievable by the CUE. When merge-sort is used, the worst-case complexity of this sorting is $\mathcal{O}(N \log N)$.
- 2) It then calculates the number of RBs required to serve the packet and identifies these RBs. According to Table IV, the maximum number of RBs required to serve a CUE packet of 50 bytes with a BLER of 0.1 is 16. So, in the worst case, GRAHS scans the first 16 RBs in the sorted list of RBs.
- 3) It checks all the VUEs to find the optimal pairing.

As a maximum of C_t users can be scheduled in a TTI, the worst case time complexity for CUE resource allocation and user pairing of GRAHS is $\mathcal{O}(C_t(N_1 \log N_1 + 16 + V))$. The Hungarian resource-sharing algorithm in GRAHS matches C_t CUEs to C_t VUEs. So, the complexity of Hungarian resource sharing is $\mathcal{O}(C_t^3)$. After pairing, the number of RBs needed individually by the CUE and the VUE packet of the pair is recalculated. Therefore, the complexity of all steps of GRAHS is $\mathcal{O}(C_t(N_1 \log N_1 + 16 + V) + C_t^3 + 2C_t)$, *i.e.*, $\mathcal{O}(C_t^3)$

In HRAHS, the resource allocation of CUEs is carried out using the Hungarian algorithm. Since a maximum of C_t users is assigned to C_t RCs, hence, the complexity of the CUE resource allocation algorithm in HRAHS is $\mathcal{O}(C_t^3)$. Again, C_t VUEs are paired with C_t CUEs using the Hungarian algorithm, and after pairing, the number of RBs needed by the VUE of each pair is recalculated. So, the combined complexity is $\mathcal{O}(2C_t^3 + V + 2C_t)$, *i.e.*, $\mathcal{O}(C_t^3)$

V. EVALUATION

In this section, we first explain the simulation parameters and then discuss the results obtained.

A. Simulation Parameters

The performances of the GRAHS and HRAHS algorithms have been validated using extensive Monte Carlo Simulations in a system-level simulator developed using Python. Each point in the figures corresponds to an average of 10 different simulation runs, each of which is 6.25 seconds long. The simulation scenario considers the service area of a single gNB to be a $1\text{km} \times 1\text{km}$ square area with the gNB at the center. We have considered eight lanes, each of width $w = 4$ metres

Table VI: Simulation Parameters

Parameter	Value
Carrier Frequency	28GHz
gNB / Vehicle antenna gain	8 dBi / 3 dBi
Simulation Area / Lane width	1 Km \times 1 Km / 4 m
Number of Lanes	4 lanes in each direction
BS / Vehicle Noise Figure	5 dB / 9 dB
Noise Power σ^2	-114 dBm
Vehicle speed	50 Kmph
Minimum spectral efficiency of CUEs r_0	0.5 bps/Hz
SINR Threshold for coverage of VUEs γ_0	5 dB
Outage probability p_0	10^{-3}
Maximum CUEs/VUEs transmit power P_c, P_v	23 dBm
Shadowing type	Log-normal
Shadowing standard deviation V_{2V} / V_{2I}	4 dB / 7.8 dB
Number of VUE Pairs / BUEs	10 / 10
Delay constraint of VUEs (δ_v)/CUE (δ_c)	10 msec / 50 msec
Packet size CUE (β_c) / VUEs (β_v)	50 bytes / 10 bytes
Packet generation rate of CUEs λ_c	Number of CUEs/20
Feedback Period T	0.125 ms

(m) and located 35m to the south of the gNB. All simulation parameters have been tabulated in Table VI. Some of the more important ones are discussed here. We have considered a high frequency of operation - 28 GHz. As mentioned before, the QoS constrained users (CUEs/CUEs+VUEs) are assigned to BWP-1 which uses numerology $\mu = 3$. The maximum number of these users scheduled in a TTI is considered to be eight. So, a minimum of eight RCs will be needed in HRAHS. Accordingly, we have taken the bandwidth of BWP-1 to be - *number of RCs* \times *number of RBs in each RC* \times *bandwidth of each RB* = $8 \times 4 \times 1440 = 46.08$ MHz. BWP-2 has a bandwidth of 3.92 MHz, a carrier frequency of 2GHz, and uses numerology $\mu = 0$. The pathloss model used for CUEs is $32.4 + 20 \log_{10}(f_c) + 30 \log_{10}(d)$ and for VUEs is $36.85 + 30 \log_{10}(d) + 18.9 \log_{10}(f_c)$ [44].

We have analyzed the performance of the proposed algorithms based on the real-time traffic capacity, which depends on the number of satisfied real-time traffic users. Real-time traffic, such as VoIP calling, video calling, video streaming, etc., are characterized by their QoS requirements, such as delay deadlines, maximum allowable packet loss rate, etc. A real-time traffic user is satisfied if (a) at least 98% of its packets are successfully delivered, *i.e.*, its packet loss ratio is less than 2%, and (b) the average packet delay is less than the delay deadline. The real-time traffic capacity is given by that number of users, out of which 95% are satisfied [35]. In this work, we have found the real-time traffic capacity for the given 5G network in terms of the number of satisfied CUEs while keeping the number of BUEs and VUE pairs constant. We have considered ten BUEs and ten VUE pairs, *i.e.*, ten VUE transmitters and ten VUE receivers.

B. Results

In this section, we have first established the need for link-adaptation by comparing the performance of GRAHS, HRAHS, and ORA with an existing algorithm [24] which assigns one RB per CUE. Subsequently, we have compared the performance of the GRAHS, HRAHS, and ORA algorithms in terms of their real-time traffic capacity, sum-rate of CUEs, and QoS performance of CUEs and VUEs.

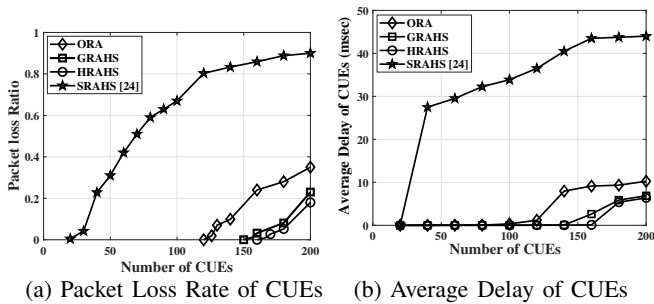


Figure 2: Comparison of ORA, GRAHS, HRAHS with baseline SRAHS [24] that has no link adaptation

1) **Need for Link Adaptation:** To establish the need for link adaptation in resource allocation, we have used the algorithm in [24], which uses the same power allocation and resource sharing as our work, but *assigns one RB per CUE*. We refer to this baseline algorithm from [24] as “*Single RB Allocation with Hungarian Sharing*” - SRAHS. While implementing SRAHS, we schedule a CUE when it needs a single RB. In other words, if the CUE has a poor channel condition and requires more than one RB, SRAHS waits till the channel condition of the CUE improves, and the user requires a single RB only. This ensures that each CUE would need one RB only, as mentioned in [24]. Fig. 2a and Fig. 2b shows the packet loss ratio and average packet delay of SRAHS, ORA, GRAHS, HRAHS, and ORA. It is observed that with SRAHS the packet loss rate of the CUEs is more than 2% when there are 25 CUEs in the system. In contrast, when link adaptation is used, the packet loss rate is around 2% even when there are more users in the system - 126 CUEs for ORA, 158 CUEs for GRAHS, and 168 CUEs for HRAHS. Although the average packet delay of SRAHS for successfully delivered packets is less than the delay bound, it remains higher than link adapted resource allocation, implying that numerous packets have been dropped due to delay bound violation. Having established the need for link adaptation, we carry out the rest of the analysis using ORA, GRAHS, and HRAHS.

2) **Performance of the CUEs:** In this section, we discuss the performance of the algorithms. Fig. 3a shows the variation of packet loss ratio with the number of CUEs, while Fig. 3b shows the Cumulative Distribution Function (CDF) of the average delay experienced by the users in milliseconds. It may be observed from Fig. 3a and Fig. 3b that the number of CUEs which meet the 2% packet loss ratio while maintaining the delay bound is 126, 158, and 168 for ORA, GRAHS, and HRAHS, respectively. So, these values are the real-time traffic capacity of the network for the given simulation scenario. ORA supports a lower real-time traffic capacity due to the dedicated resource assignment for which the limit on the maximum number of users scheduled in a TTI is applicable to both the CUEs and VUEs. The supported capacity increases with resource sharing between CUEs and VUEs. Furthermore, the capacity of HRAHS is even higher than GRAHS. GRAHS and HRAHS allocate resources to users in the order they appear in the TTL-sorted buffers. The following two conditions may arise with GRAHS: - 1) If users with poor channel conditions are ahead in the queue, they will occupy a larger number of RBs thereby throttling resource availability

to the trailing users. 2) If users with poor channel conditions appear later in the queue, then a sufficient number of resources may not be available. As GRAHS aims to maximize the sum rate, it implicitly prioritizes users with better channel conditions, *i.e.*, fewer resource requirements. This can be corroborated from Fig. 5b, which plots the average number of RBs required by each CUE per TTI. It is seen from Figs. 5a and 5b that GRAHS occupies fewer resources. In fact, the percentage of users requiring 1/2/3/4 RBs with GRAHS varies as 59%/14%/15%/4.78%, respectively. HRAHS, on the other hand, universally assigns four RBs per user, thereby supporting users even with average channel conditions. As a result, the real-time traffic capacity of HRAHS is 168 CUEs, which is even higher than that of GRAHS at 158 CUEs.

Fig. 3b shows the comparison of the delay performance of the three algorithms at two levels - (i) for the same number of users, and (ii) for the real-time traffic capacity of individual algorithms. For comparing the performance with the same number of users, we have used the real-time traffic capacity of ORA of 126 users, which is the least among all the algorithms. It is observed that with the same number of users, ORA delivers the worst delay performance among all algorithms. The reason can also be attributed to the fact that for ORA the limit on the maximum number of users that can be scheduled in a TTI applies to both CUEs and VUEs. When the delay performance is compared at the capacity of individual algorithms, it is seen that the delay experienced with GRAHS and HRAHS increases with the number of CUEs, but it is well within the maximum allowable delay of 50ms.

Fig. 3c compares the sum-rate achieved by the three different algorithms for 126 CUEs, *i.e.*, for the real-time traffic capacity of the ORA algorithm. It is seen that HRAHS is able to provide a much higher sum-rate for the CUEs, than GRAHS. HRAHS achieves the higher system capacity and improved sum-rates by efficient utilization of the radio resources. The resource utilization of the three algorithms can be observed from Fig. 5a, which shows the number of RBs occupied by the CUEs. It shows that HRAHS has a better resource utilization, which gets reflected in the improved capacity and sum rates.

3) **Performance of the VUEs:** Fig. 4 shows the performance of the VUEs under the different resource allocation schemes. In ORA, both CUEs and VUEs are sorted in the same buffer according to their time-to-live. As VUE packets have a shorter TTL, hence when generated in the same TTI, VUE packets will have a higher priority than CUEs. As the ORA algorithm implicitly prioritizes VUEs over CUEs, hence it is observed from Fig. 4a that the VUEs will experience least delay when being scheduled with ORA. However, it comes at the cost of increased outage probability as seen in Fig. 4b. This is because in TTIs where the CUE packets have a higher priority, they will occupy a larger number of RBs due to their larger packet size. This will throttle the availability of bandwidth to the trailing VUEs. In addition, if these VUEs have a poorer channel condition then the number of RBs needed to serve the packet may not be available, resulting in the higher outage probability. On the other hand, when the RBs are shared, as in GRAHS and HRAHS, the VUEs have

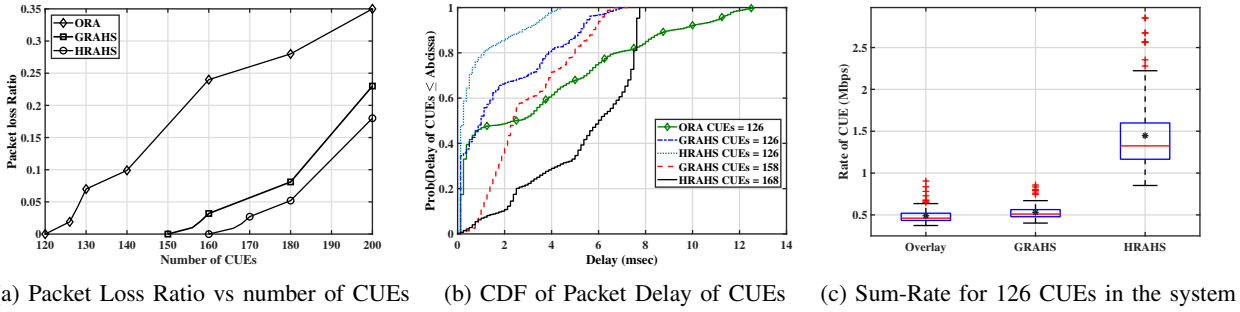


Figure 3: Performance of the different Resource allocation algorithms in terms of Packet Loss Rate, Average Delay, Sum-Rate experienced by the CUEs

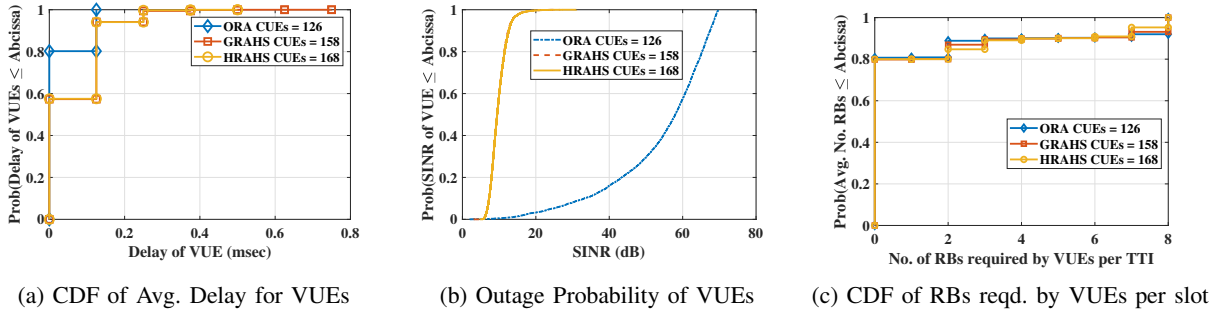


Figure 4: Performance of the different Resource allocation algorithms in terms of the Average Delay, Outage Probability, and the RB requirement of VUEs

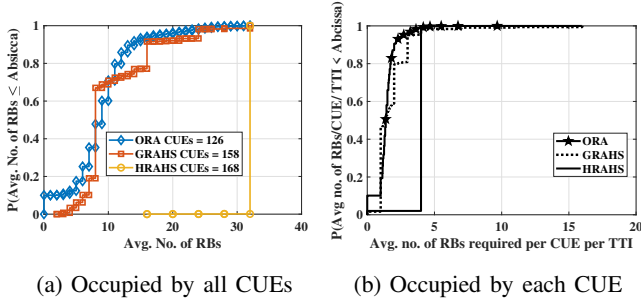


Figure 5: CDF of the Number of RBs occupied by the CUEs. The CDF has been shown for the number of RBs occupied by all CUEs as well as per CUEs.

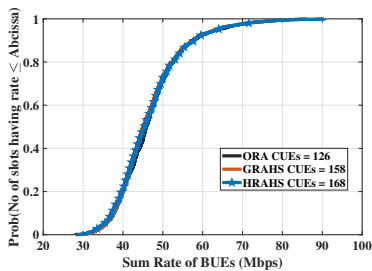


Figure 6: CDF of the rate of the best effort users

access to a larger number of RBs, resulting in the improved outage probability performance. Fig. 4c shows the resource utilization of the VUEs. It remains fairly constant for all the algorithms as the number of VUEs remain constant.

4) *Performance of the BUEs:* Fig. 6 shows CDF of the sum-rate of the BUEs. For all the three algorithms, the BUEs have been scheduled using MAX C/I algorithm in which each RB is assigned to that CUE which supports the highest rate. As the bandwidth, resource allocation, and the number of BUEs remain unchanged, hence, the CDF performance remains the same for all the three cases. The existence of the BUEs necessitates the use of multiple numerologies.

Therefore, we may infer that link adaptation is indispensable for serving a combined subscriber base of V2I and V2V users in a C-V2X system operating with 5G technology.

VI. CONCLUSION

In this work, we have asserted the need for link adaptation in spectrum allocation of Cellular Vehicle-to-Everything (C-V2X) systems. This work aims to increase the number of Vehicle-to-Infrastructure (V2I) users for a given number of Vehicle-to-Vehicle (V2V), and best-effort users. The diverse Quality of Service (QoS) requirements of these users have been provided using the multi-numerology-based frame structure of 5G. The V2V users operate in underlaid mode, sharing resources with the V2I users. In contrast to existing works, our method assumes that the number of Resource Blocks (RBs) required by the users is a function of their underlying channel conditions and QoS requirements. Our first algorithm, called GRAHS, assigns resources to users using a greedy method, and the second one assigns resources to V2I users using the Hungarian method. In their second stage, both algorithms use the Hungarian algorithm for optimal pairing between V2V and

V2I users. We have observed that link adaptation significantly improves the QoS provisioning, and, hence, the supported real-time traffic capacity of the systems.

In this work, we have considered all users to have a constant velocity and have aimed to maximize the V2I links only. As a future extension, we plan to design lower computationally complex resource allocation algorithms, which in addition to increasing the number of V2I users will also aim to increase the number of V2V links for different mobility conditions. Furthermore, these resource allocation algorithms will also aim to use fewer resources for the QoS-constrained users to improve the sum rate of the best-effort users.

REFERENCES

- [1] P. K. Korrai, E. Lagunas, A. Bandi, S. K. Sharma, and S. Chatzinotas, "Joint Power and Resource Block Allocation for Mixed-Numerology-Based 5G Downlink Under Imperfect CSI," *IEEE Open Journ. of Comm. Society*, vol. 1, pp. 1583–1601, 2020.
- [2] K. Ganesan, J. Lohr, P. B. Mallick, A. Kunz, and R. Kuchibhotla, "NR Sidelink Design Overview for Advanced V2X Service," *IEEE Internet of Things Mag.*, vol. 3, no. 1, pp. 26–30, 2020.
- [3] M. H. C. Garcia, A. Molina-Galan, M. Boban, J. Gozalvez, B. Coll-Perales, T. Şahin, and A. Kousaridas, "A Tutorial on 5G NR V2X Communications," *IEEE Commun. Surveys & Tutorials*, vol. 23, no. 3, pp. 1972–2026, 2021.
- [4] X. Zhang, L. Zhang, P. Xiao, D. Ma, J. Wei, and Y. Xin, "Mixed numerologies interference analysis and inter-numerology interference cancellation for windowed ofdm systems," *IEEE Trans. on Vehicular Tech.*, vol. 67, no. 8, pp. 7047–7061, 2018.
- [5] 3GPP, "NR; Physical channels and modulation," TS 38.211, Apr. 2022, Release 15.
- [6] P. Guan, D. Wu, T. Tian, J. Zhou, X. Zhang, L. Gu, A. Benjebbour, M. Iwabuchi, and Y. Kishiyama, "5g field trials: Ofdm-based waveforms and mixed numerologies," *IEEE Journal on Selected Areas in Communications*, vol. 35, no. 6, pp. 1234–1243, 2017.
- [7] H. Son, G. Kwon, H. Park, and J. S. Park, "Massive MIMO Precoding for Interference-Free Multi-Numerology Systems," *IEEE Trans. Vehicular Tech.*, vol. 71, no. 9, pp. 9765–9780, 2022.
- [8] L.-H. Shen, C.-Y. Su, and K.-T. Feng, "Comp enhanced subcarrier and power allocation for multi-numerology based 5g-nr networks," *IEEE Trans. Vehicular Tech.*, vol. 71, no. 5, pp. 5460–5476, 2022.
- [9] Y. Ren, F. Liu, Z. Liu, C. Wang, and Y. Ji, "Power Control in D2D-Based Vehicular Communication Networks," *IEEE Trans. on Vehicular Tech.*, vol. 64, no. 12, pp. 5547–5562, 2015.
- [10] X. Li, R. Shankaran, M. Orgun, L. Ma, and Y. Xu, "Joint Autonomous Resource Selection and Scheduled Resource Allocation for D2D-Based V2X Communication," in *IEEE VTC*, 2018, pp. 1–5.
- [11] X. Li, L. Ma, R. Shankaran, Y. Xu, and M. A. Orgun, "Joint Power Control and Resource Allocation Mode Selection for Safety-Related V2X Communication," *IEEE Trans. Vehicular Tech.*, vol. 68, no. 8, pp. 7970–7986, 2019.
- [12] Z. He, L. Wang, H. Ye, G. Y. Li, and B.-H. F. Juang, "Resource Allocation based on Graph Neural Networks in Vehicular Communications," in *IEEE Globecom*, 2020, pp. 1–5.
- [13] C. He, Q. Chen, C. Pan, X. Li, and F.-C. Zheng, "Resource Allocation Schemes Based on Coalition Games for Vehicular Communications," *IEEE Comm. Lett.*, vol. 23, no. 12, pp. 2340–2343, 2019.
- [14] M. Chen, J. Chen, X. Chen, S. Zhang, and S. Xu, "A Deep Learning Based Resource Allocation Scheme in Vehicular Communication Systems," in *IEEE WCNC*, 2019, pp. 1–6.
- [15] Y. Hou, X. Wu, X. Tang, X. Qin, and M. Zhou, "Radio Resource Allocation and Power Control Scheme in V2V Communications Network," *IEEE Access*, vol. 9, pp. 34 529–34 540, 2021.
- [16] T. Liu, L. Lei, K. Zheng, Xuemin, and Shen, *Multi-timescale control and communications with deep reinforcement learning – part i: Communication-aware vehicle control*, 2023.
- [17] L. Liang, G. Y. Li, and W. Xu, "Resource Allocation for D2D-Enabled Vehicular Communications," *IEEE Trans. Comm.*, vol. 65, no. 7, pp. 3186–3197, 2017.
- [18] C. Guo, L. Liang, and G. Y. Li, "Resource Allocation for Low-Latency Vehicular Communications with Packet Retransmission," in *IEEE Globecom*, 2018, pp. 1–6.
- [19] C. Guo, L. Liang, and G. Y. Li, "Resource Allocation for Low-Latency Vehicular Communications: An Effective Capacity Perspective," *IEEE JSAC*, vol. 37, no. 4, pp. 905–917, 2019.
- [20] C. Guo, L. Liang, and G. Y. Li, "Resource Allocation for High-Reliability Low-Latency Vehicular Communications With Packet Retransmission," *IEEE Trans. Vehicular Tech.*, vol. 68, no. 7, pp. 6219–6230, 2019.
- [21] W. Sun, D. Yuan, E. G. Ström, and F. Brännström, "Cluster-Based Radio Resource Management for D2D-Supported Safety-Critical V2X Communications," *IEEE Trans. Wireless Commun.*, vol. 15, no. 4, pp. 2756–2769, 2016.
- [22] S. Gyawali, Y. Qian, and R. Q. Hu, "Resource Allocation in Vehicular Communications Using Graph and Deep Reinforcement Learning," in *IEEE Globecom*, 2019, pp. 1–6.
- [23] W. Wu, R. Liu, Q. Yang, and T. Q. S. Quek, "Robust Resource Allocation for Vehicular Communications With Imperfect CSI," *IEEE Trans. Wireless Comm.*, vol. 20, no. 9, pp. 5883–5897, 2021.
- [24] L. Liang, J. Kim, S. C. Jha, K. Sivanesan, and G. Y. Li, "Spectrum and Power Allocation for Vehicular Communications With Delayed CSI Feedback," *IEEE Wireless Comm. Lett.*, vol. 6, no. 4, pp. 458–461, 2017.
- [25] X. Li, L. Ma, Y. Xu, and R. Shankaran, "Resource Allocation for D2D-Based V2X Communication With Imperfect CSI," *IEEE Internet of Things Journal*, vol. 7, no. 4, pp. 3545–3558, 2020.
- [26] D. Ron and J.-R. Lee, "Dnn-based dynamic transmit power control for v2v communication underlaid cellular uplink," *IEEE Trans. on Vehicular Tech.*, vol. 71, no. 11, pp. 12 413–12 418, 2022.
- [27] G. Chai, W. Wu, Q. Yang, R. Liu, and F. R. Yu, "Learning-based resource allocation for ultra-reliable v2x networks with partial csi," *IEEE Trans. on Commun.*, vol. 70, no. 10, pp. 6532–6546, 2022.
- [28] G. Chai, W. Wu, Q. Yang, and F. R. Yu, "Data-Driven Resource Allocation and Group Formation for Platoon in V2X Networks With CSI Uncertainty," *IEEE Trans. Commun.*, pp. 1–1, 2023.
- [29] R. Aslani, E. Saberinia, and M. Rasti, "Resource allocation for cellular v2x networks mode-3 with underlay approach in lte-v standard," *IEEE Trans. on Vehicular Tech.*, vol. 69, no. 8, pp. 8601–8612, 2020.
- [30] Z. Liu, J. Su, Y.-a. Xie, K. Ma, Y. Yang, and X. Guan, "Resource allocation in d2d enabled vehicular communications: A robust stackelberg game approach based on price-penalty mechanism," *IEEE Trans. on Vehicular Tech.*, vol. 70, no. 8, pp. 8186–8200, 2021.
- [31] F. J. Martín-Vega, J. C. Ruiz-Sicilia, M. C. Aguayo, and G. Gómez, "Emerging Tools for Link Adaptation on 5G NR and Beyond: Challenges and Opportunities," *IEEE Access*, vol. 9, pp. 126 976–126 987, 2021.
- [32] D. B. West, *Introduction to Graph Theory*, 2nd ed. Prentice Hall, Sep. 2000.
- [33] F. D. Calabrese, P. H. Michaelsen, C. Rosa, M. Anas, C. Ubeda Castellanos, C. U. Castellanos, D. L. Villa, K. I. Pedersen, and P. E. Mogensen, "Search-Tree Based Uplink Channel Aware Packet Scheduling for UTRAN LTE," in *IEEE VTC*, 2008, pp. 1949–1953.
- [34] A. Mukhopadhyay, G. Das, and V. Sudheer Kumar Reddy, "A fair uplink scheduling algorithm to achieve higher MAC layer throughput in LTE," in *IEEE ICC*, 2015, pp. 3119–3124.
- [35] B. Palit and S. S. Das, "Performance evaluation of mixed traffic schedulers in OFDMA networks," *Wireless Pers. Commun.*, vol. 83, no. 2, pp. 895–924, 2015.
- [36] B. Ji, B. Dong, D. Li, Y. Wang, L. Yang, C. Tsimenidis, and V. G. Menon, "Optimization of Resource Allocation for V2X Security Communication based on Multi-Agent Reinforcement Learning," *IEEE Trans. on Vehicular Tech.*, pp. 1–12, 2023.
- [37] 3GPP, "Study on LTE-based V2X services," TR 36.885, Jun. 2016, release 14.
- [38] G. L. Stuber, *Principles of Mobile Communication*, 1st. USA: Kluwer Academic Publishers, 1996.
- [39] 3GPP, "NR; Physical channels and modulation," TS 38.211, Mar. 2024, Release 15.
- [40] 3GPP, "NR; User Equipment (UE) radio transmission and reception; Part 1: Range 1 Standalone," TS 38.101, Apr. 2024, Release 18.
- [41] 3GPP, "NR; Physical layer procedures for data," TS 38.214, Mar. 2024, Release 18.
- [42] E. Dahlman, S. Parkvall, and J. Skold, *4G, LTE-Advanced Pro and The Road to 5G, Third Edition*, 3rd. USA: Academic Press, Inc., 2016.
- [43] E. Dahlman, S. Parkvall, and J. Skold, *4G: LTE/LTE-advanced for mobile broadband*. Academic press, 2013.
- [44] 3GPP, "Study on evaluation methodology of new Vehicle-to-Everything (V2X) use cases for LTE and NR," TS 37.885, Jun. 2019, release 15.

This figure "fig1.png" is available in "png" format from:

<http://arxiv.org/ps/2305.02667v3>